Taylor & Francis
Taylor & Francis Group

Spectroscopy Letters

An International Journal for Rapid Communication

ISSN: 0038-7010 (Print) 1532-2289 (Online) Journal homepage: www.tandfonline.com/journals/lstl20

Surface Acidity of H-Birnessite: Infrared Spectroscopic Study of Formic Acid Decomposition

E. Eren, H. Gumus, B. Eren & A. Sarihan

To cite this article: E. Eren, H. Gumus, B. Eren & A. Sarihan (2013) Surface Acidity of H-Birnessite: Infrared Spectroscopic Study of Formic Acid Decomposition, Spectroscopy Letters, 46:1, 60-66, DOI: 10.1080/00387010.2012.666612

To link to this article: https://doi.org/10.1080/00387010.2012.666612

Published online: 03 Jan 2013.

Submit your article to this journal

Article views: 255

View related articles

Citing articles: 1 View citing articles

Full Terms & Conditions of access and use can be found at
https://www.tandfonline.com/action/journalInformation?journalCode=lstl20

Spectroscopy Letters, 46:60–66, 2013
Copyright © Taylor & Francis Group, LLC
ISSN: 0038-7010 print/1532-2289 online
DOI: 10.1080/00387010.2012.666612

Taylor & Francis
Taylor & Francis Group

Surface Acidity of H-Birnessite: Infrared Spectroscopic Study of Formic Acid Decomposition

E. Eren,
H. Gumus,
B. Eren,
and A. Sarihan

Bilecik University, Faculty of Arts and Science, Department of Chemistry, Bilecik Turkey

ABSTRACT This paper presents the adsorption and thermal decomposition mechanism of formic acid on an H-birnessite sample. Changes in the surface and structure were characterized using infrared spectroscopy, N_2 gas adsorption–desorption, and thermal analysis techniques. The acid sites of H-birnessite were investigated by infrared and thermal analysis using pyridine as a molecular probe. Decomposition of formic acid started on H-birnessite at 120°C and was complete at 400°C. Infrared spectra revealed that the molecularly adsorbed formic acid species were transformed to a formate species, and the formate species were transformed to CO. The most stable adsorption structure for formic acid was found as a molecular monodentate configuration.

KEYWORDS birnessite, manganese oxide, Mn_2O_3, Mn_3O_4, MnO_2, surface acidity

INTRODUCTION

The acidic and basic properties of oxide catalysts are very important for the development of scientific criteria in catalyst applications. The determination of the strength of acidic and basic sites exposed on the solid surface as well as their distribution is a necessary requirement to understand the catalytic properties of solid acids and bases. A complete description of acidic and basic properties of solid surface requires the determination of acidic and base strength, acidic or base amount, and nature of such sites.

Decomposition of formic acid is a classic reaction in heterogeneous catalysis. The selectivity in formic acid decomposition is used for characterizing acid–base properties of oxide catalysts: dehydration takes place on acidic oxides, whereas dehydrogenation occurs on basic ones. On the surface of the majority of oxide catalysts, formic acid is adsorbed dissociatively with the formation of surface formates.[1] Formate ions stabilized on Lewis acid sites have been shown to be intermediates in formic acid decomposition via the dehydrogenation mechanism.[1] Formic acid dehydration takes place both on Bronsted acid sites with the participation of protons and on aprotic sites via intermediate surface formates.[1]

Received 13 December 2011; accepted 10 February 2012.

Address correspondence to E. Eren, Bilecik University, Faculty of Arts and Science, Department of Chemistry, 11210, Bilecik Turkey. E-mail: erdal.eren@bilecik.edu.tr

Manganese can form a number of oxides due to the different oxidation states. Birnessite-type compounds are nonstoichiometric manganese oxides. The generic name corresponds to mixed oxides formed by the well-organized arrangement of octahedral MnO_6 layers. The Mn^{n+} average oxidation state is below IV, which corresponds to a basic structure of Mn(IV) with substitution of some Mn ions for Mn(III) and even Mn(II).[2,3] This complex chemistry provides interesting catalytic properties to the manganese oxides.[4–6] Among manganese oxides, birnessite has demonstrated high catalytic activity for different reactions such as the selective catalytic reduction of NOx with NH_3,[7] the catalytic decomposition of ozone,[8] or the catalytic combustion of volatile organic compounds.[9]

The determination of the structures of organic molecules adsorbed on surfaces is one of the determining factors in the efficiency of the decomposition process. The adsorption geometry of the organic molecules is of crucial importance for the stability of adsorbed organic compounds. Because infrared (IR) spectroscopy is sensitive to small structural changes, it has been widely used to study the adsorption geometry of small organic molecules adsorbed to surfaces and to follow reaction mechanisms on surfaces.[10–16]

A careful analysis of the existing literature indicates that not many studies have been conducted for understanding the decomposition pathway of formic acid using manganese oxides. Taking into account this background, H-birnessite was synthesized and evaluated in the decomposition of formic acid under atmospheric pressure. IR desorption studies of formic acid on H-birnessite were performed to get better insight into the decomposition mechanism. Also, the acid sites of H-birnessite were investigated by IR spectroscopy and thermal analysis (TA) techniques using pyridine as a molecular probe.

EXPERIMENTAL

Materials and Methods

All reagents, such as aniline, KNO_3, $KMnO_4$, HNO_3, NaOH, and $Mn(NO_3)_3{\cdot}9H_2O$, were of analytical grade and all solutions were prepared with double-distilled water. K-birnessite was prepared according to the redox method described in the literature.[17] The K-birnessite was treated with a 1-M HNO_3 solution for 24 hr at room temperature, then washed with distilled water and dried at 70°C, which was designated as H-birnessite.

IR spectra of the birnessite samples were recorded in the region 4000–450 cm^{-1} on a Spectrum-100 FTIR spectrometer. The thermal gravimetric (TG) and differential thermal analyses (DTA) curves were obtained using a PRIS Diamond TG/DTG apparatus under highly pure nitrogen atmosphere (N_2 flow rate: 20 cm^3/min, heating rate: 10°C min^{-1}, platinum crucibles, mass ~10 mg, and temperature range: 30–1000°C). A Tri Star 3000 (Micromeritics, USA) surface analyzer was also used to measure the nitrogen adsorption isotherm at 77 K in the range of relative pressure 10^{-6} to 1. Before measurement, the sample was degassed at 300°CC for 2 hr. The surface areas were calculated by the BET (Brunauer–Emmett–Teller) method. The XRD analysis data from the samples were collected using a Rigaku, Miniflex ZD13113 (Japan) diffractometer with Cu Kα radiation with Ni filter.

The Brønsted and Lewis acid sites were determined by IR spectroscopy with chemisorbed pyridine. For this purpose, birnessite samples were dried in a hot-air oven for 24 hr at 120°C prior to pyridine treatment for IR measurements. The samples (50 mg each) were poured loosely into a sample cup. The loosely filled sample was brought in contact with pyridine (0.1 cm^3) directly. Then the sample cup was kept in a hot-air oven at 100°C for 1 hr to remove physisorbed pyridine. After cooling down to room temperature and adsorption of pyridine, the sample-adsorbed pyridine was evacuated for 20 min at several temperatures (373°C, 200°C, 300°C, 400°C). Specimens for measurement were prepared by mixing 0.9 mg of the sample powder with 70 mg of KBr and pressing the mixture into a pellet.

The interaction between gas-phase formic acid and birnessite surface was accomplished in desiccators for 2 hr at room temperature. After adsorption studies, desorption experiments were also done at elevated temperatures (373–400°C) for 10 min.

RESULTS AND DISCUSSION

Material Characterization

Figures 1a and b show the IR spectra of the K-birnessite and H-birnessite samples between 4000 and 450 cm^{-1}. In the IR spectrum of the K-birnessite

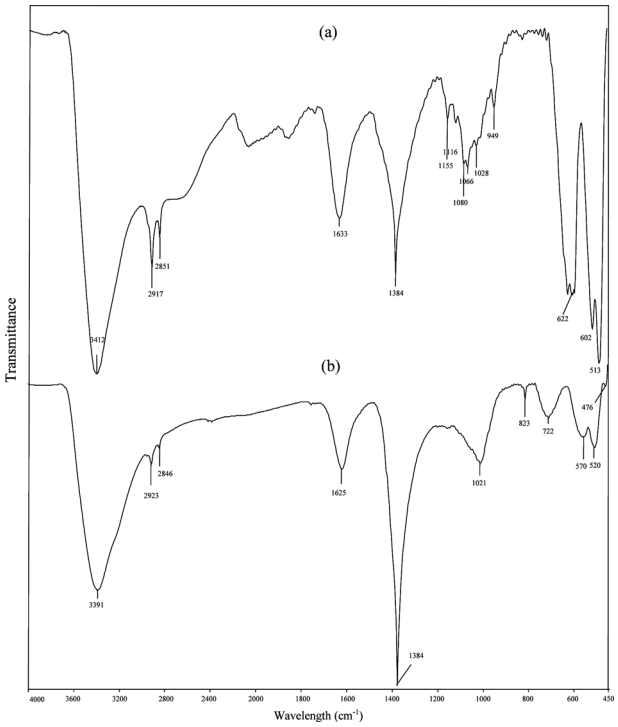

FIGURE 1 **IR spectra of the K-birnessite (a) and H-birnessite (b) samples.**

sample, the broad peak at 3412 cm^{-1} is due to stretching vibrations of its interlayer hydrates.[18] For the K-birnessite sample, two strong IR bands could be observed around 513 and 602 cm^{-1}, in good agreement with the IR characteristic bands of birnessites.[19–21] Several absorption bands were observed at 3391, 2923, 2846, 1633, 1384, 1024, 823, 722, 570, and 520 cm^{-1} in the IR spectrum of the H-birnessite sample. Three bands located within the 2800–3500 cm^{-1} region are confirmed to be due to the components of the asymmetric and symmetric stretching modes of the H_2O molecule. The 3391 cm^{-1} band was attributed to stretching vibrations of the O-H group of water molecules and the lattice hydroxyl groups or H_3O^+, and less-ordered water produces the remaining features at 2923 and 2846 cm^{-1} and a broad band at 1633 cm^{-1}, which supports the argument that interlayer water exists in H-birnessite.[22] Some changes were detected in the region between 400 and 800 cm^{-1}, which assigned to Mn-O lattice vibration.[19–21]

The characteristics of the porous structure, including the BET surface area, the pore volume, and the pore size, obtained from the conventional nitrogen isotherm analysis are presented in Table 1. As shown in Table 1, H-birnessite has a higher surface area and total pore volume and a lower micropore volume than K-birnessite. The potassium ions may screen out some of the birnessite surface roughness, which becomes inaccessible for the nitrogen molecules and then decreases the BET surface area. Another possibility leading to the reduction of the BET surface area comes from the fact that potassium cation may clog some of the smaller pores; that is, the pore-blocking effect occurs. The XRD study on H-birnessite indicated that the layered structure was retained, and almost no change was observed on the basal spacing of the layered structure after the acid activation process.

Surface Acidity of H-Birnessite Sample

Adsorption of pyridine as a base on the surface of solid acids is one of the most frequently applied methods for the characterization of surface acidity. The IR spectra in the spectral region 1400 and 1700 cm^{-1} after pyridine treatment and thermal desorption at different temperatures for 20 min of pyridine adsorbed on H-birnessite are presented in Fig. 2. The IR absorption bands were assigned according to the literature.[23–25] After heating at 120°C, important pyridine vibrations were observed at 1633, 1620, 1601, 1572, 1542, 1508, 1485, 1474, and 1442 cm^{-1}. In Fig. 2, the attention should be focused on the high-temperature region because at low temperatures the information about the Lewis sites is obscured by the band of hydrogen-bonded pyridine. The band at 1434 cm^{-1} is stable to heating at 500°C (Fig. 2). This indicated that this band was

TABLE 1 **Porous Structure Parameters of the K-Birnessite and H-Birnessite Samples**

Sample	S_{BET} (m^2/g)	S^a_{ext} (m^2/g)	S_{mic} (m^2/g)	V_t (cm^3/g)	V_{mic} (cm^3/g)	D^b_p (nm)
K-birnessite	34	29	5	0.169	0.0027	19.79
H-birnessite	42	39	3	0.210	0.0015	19.84

[a] $S_{ext} = S_{meso}$.
[b] 4 V/A by BET.

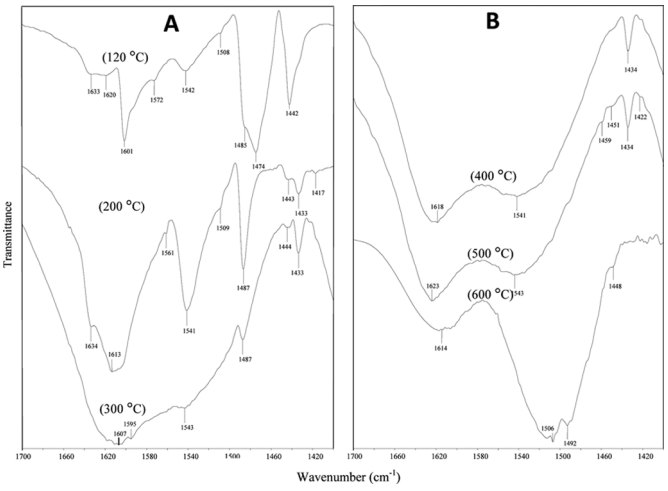

FIGURE 2 **Desorption of pyridine from H-birnessite, after thermal treatments between 120°C and 600°C.**

not assignable to hydrogen-bonded pyridine on H-birnessite, which is unstable to outgassing at temperatures as low as 120°C. This band can be attributed to the ring-stretching vibration of pyridine coordinately bonded to the Lewis acid centers.[25] In addition, the intensive band at 1620 cm^{-1} suggested the presence of Lewis acid centers and the band near 1542 cm^{-1} of high intensity signified the presence of a relatively large amount of Brønsted acid sites.[25] These species were formed as pyridinium ions, with a transfer of H^+ ion from the Brønsted acidic -OH_2^+ groups of the H-birnessite to pyridine. Pyridine bands at 1601 and 1620 cm^{-1} indicated two types of pyridine, which directly coordinated with the adsorption sites on H-birnessite. After thermal activation at 200°C, the very broad band was observed near 1633 cm^{-1} including vibration of water and interaction of pyridine with the Lewis sites. The band at 1487 cm^{-1} was attributed to pyridine associated with both Lewis and Brønsted acid sites. After heating at 300°C, a significant amount of pyridine remained on Lewis acid sites of the H-birnessite. However, the intensity of the Brønsted band at 1541 cm^{-1} was reduced significantly. After heating at 500°C, the intensities of the bands assigned to pyridine adsorbed on Lewis sites at 1618 and 1434 cm^{-1}, however, were still significant.

The thermal stability of the H-birnessite sample was investigated by DTA-TG (Fig. 3a). The curve relating to the H-birnessite sample exhibited mass loss 16.6% at 20–200°C and 17.1% at 200–1000°C (Fig. 3a). This material has endothermic peaks

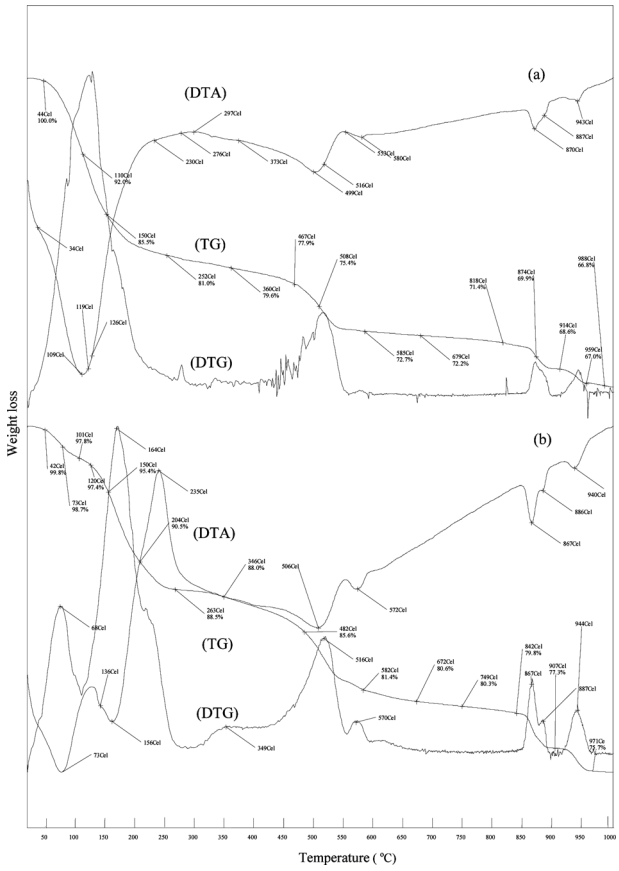

FIGURE 3 **Thermal analysis curves of the H-birnessite (a) and H-birnessite/pyridine (b) samples.**

around 109°C, 499°C, 580°C, 870°C, and 943°C, each corresponding to a weight loss, and an exothermic peak around 553°C was detected, as shown in Fig. 3b. The endothermic peak at 109°C corresponds to the evaporation of (surface) adsorbed water in the H-birnessite. The other endothermic peaks around 499°C, 870°C, and 943°C were assigned to the partial transformation of the H-birnessite phase to Mn_2O_3 (release of oxygen from the H-birnessite phase), transformation of an Mn_2O_3 phase to Mn_3O_4 phase (associated with the release of oxygen), and collapsing of the H-birnessite, respectively.[26,27] The exothermic peak without weight change at 553°C corresponds to a structural transformation reaction from the layered structure of H-birnessite to the tunnel structure (cryptomelane).[21,26,27] As shown in Fig. 3, the TG curve for H-birnessite shows approximately smooth mass loss in the range of temperatures between 580°C and 818°C. This indicated that the structure of the H-birnessite sample was stable. Also, the stable range of thermogram between 580°C and 818°C indicated that both the manganese

oxide phases (i.e., MnO_2 and Mn_2O_3) coexist with a very slow transition toward Mn_3O_4.[26,27] The endothermic peak at 870°C for H-birnessite was assigned to the phase transformation of Mn_2O_3 to Mn_3O_4. In the H-birnessite sample, the lower temperature for Mn_3O_4 formation may be attributed to the lattice irregularities and dislocations within the crystals.

Thermal desorption of pyridine was also followed by thermal analyses to estimate the acid strength of both Brønsted and Lewis acid centers. Thermal analysis techniques may provide a simple and effective tool to understand and control catalysts' quality. The amounts of pyridine desorbed can be divided into three temperature ranges to denote three types of acid sites: (1) weak acid sites ranging from 100°C to 250°C, (2) moderate acid strength, ranging from 250°C to 400°C, and (3) high acid strength, ranging from 400°C to 600°C. The total of mass losses up to 1000°C is 24.7% for the pyridine-adsorbed H-birnessite sample (Fig. 3b). The endothermic peak at 156°C for H-birnessite is associated largely with weakly chemisorbed pyridine molecules rather than physically adsorbed pyridine molecules. The total of mass losses up to 250°C is 11.2% for H-birnessite samples. This peak is associated with pyridine molecules adsorbed on H-birnessite hydroxyl groups (the Brønsted acid sites). High desorption at low temperatures could be due to the interaction of pyridine with weakly acidic sites in sample. No desorption maximum from acid sites was observed in the range of temperature between 250°C and 400°C for the H-birnessite sample, suggesting absence of the sites of moderate acid strength.

Desorption of Formic Acid from H-Birnessite

IR spectra in the absorption mode are shown in Fig. 4. IR bands are assigned according to the literature.[28–32] The first spectrum in Fig. 4 shows the infrared absorptions measured after desorption of formic acid on H-birnessite at 120°C, with peaks or shoulders at 1326, 1392, 1562, 2191, 2905, 2997, 3276, and 3351 cm^{-1}. The bands observed within 1800–1200 cm^{-1} are related to OCO stretching vibration. The bands in this region arise from surface carbonates or the formate species. The formation of formate can be detected by analyzing the C-H stretching vibration region (set of bands at around

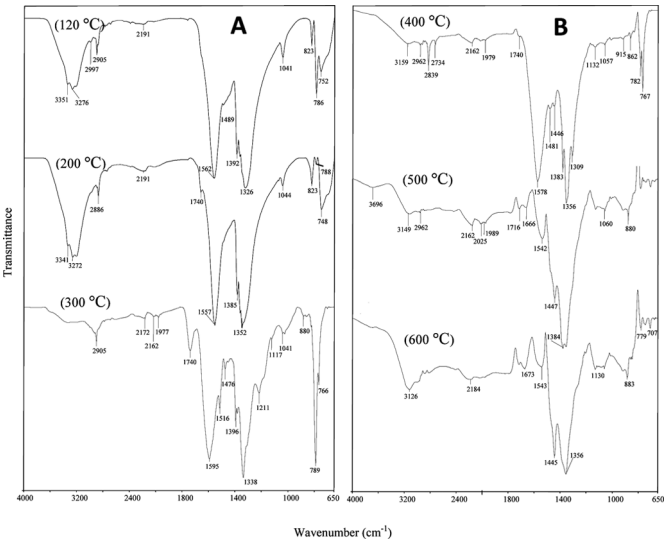

FIGURE 4 **IR spectra of formic acid species adsorbed on H-birnessite, after thermal treatments samples between 120°C and 600°C.**

2900 cm^{-1}). At 120°C, the C-H stretching vibrations confirming the generation of formate species were observed at 2905 and 2997 cm^{-1}. These two bands (at 2905 and 2997 cm^{-1}) are possibly due to the C-H stretching of formate species having different adsorption geometries. The related C-H stretching vibrations at 2800–2900 cm^{-1} were also observed with increasing the temperature values from 200°C to 400°C. On heating at 500°C, the high-frequency bands at 2940–2830 cm^{-1} became much smaller and were no longer observable above 600°C (Fig. 4). After heating at 200°C, the COO^- asymmetric peak shifted from 1562 to 1557 cm^{-1}, and the COO^- symmetric peak shifted from 1326 to 1352 cm^{-1}.[33] After increasing the temperature, an increase in the intensities of absorption bands in the 2200–1800 cm^{-1} range, corresponding to surface CO species, was observed. The 2191 cm^{-1} absorption started to appear at 120°C, indicating that some of the surface formic acid molecules decomposed.[34] The appearance of this band can be accepted as indirect proof of the decomposition of formic acid. On heating to 300°C, the characteristic bands of chemisorbed CO at 2172, 2162, and 1977 cm^{-1} grew up. Bands at 2172 and 2162 cm^{-1} can be attributed to terminal, mono-coordinated, or linearly bonded carbon monoxide, while the broad, convoluted bands at 1997 cm^{-1} are assigned to multicoordinated CO.[34] In the 300°C spectrum, the carbonyl peak was located at 1740 cm^{-1} and its intensity further

increased as compared to that in the 200°C spectrum. Meanwhile, the 1386 cm^{-1} intensity diminished and the peak shape for the absorption near 1338 cm^{-1} also varied. These temperature-dependent results indicate that a chemical transformation of the surface formic acid is under way. Heating from 200°C to 300°C and then further to 400°C clearly illustrated the decomposition and desorption of the remaining formic acid as determined by the disappearance of the carbonyl stretching mode at 1740 cm^{-1}. Simultaneously, the amount of formate reached a maximum at 300°C and then diminished slightly by 400°C as seen by the changes of intensity of features at 1309 and 1740 cm^{-1}. Formate also decomposed within the temperature range of 300–400°C to adsorb CO as suggested by the shift of 1973 to 1979 cm^{-1}. At 300°C, the 1740 cm^{-1} is due to carbonyl absorption, but it is red-shifted as compared to the 1770 cm^{-1} observed for the isolated formic acid gas molecules.[28,32] The shift of the carbonyl band toward lower frequency arose from its interaction with surface Lewis acid sites (Mn ions) or OH groups through the lone pair on the oxygen atom. After heating the sample to 300°C, the peak at 1595 cm^{-1} broadened to include a smaller peak at 1516 cm^{-1}, as shown in Fig. 4.

Mechanism of Decomposition Reaction

The difference in OCO antisymmetric and symmetric stretching frequencies of formate ($\Delta\nu_{as\text{-}s}$) relative to the aqueous ionic formate ($\Delta\nu_{ionic} = 201\ cm^{-1}$) can reveal formate bonding geometries on surfaces.[30,35–38] The correlations between $\Delta\nu_{as\text{-}s}$ and adsorption geometry have been described as follows:[30] $\Delta\nu_{as\text{-}s} > \Delta\nu_{ionic}$ = monodentate coordination; $\Delta\nu_{as\text{-}s} < \Delta\nu_{ionic}$ = chelating or bidentate bridging; $\Delta\nu_{as\text{-}s} << \Delta\nu_{ionic}$ = bidentate chelating. After heating at 120°C, the $\Delta\nu_{as\text{-}s}$ is 236 cm^{-1} in Fig. 4, indicating that monodentate formate is on the surface.

CONCLUSION

The influence of temperature on formic acid decomposition was also investigated in detail. From pyridine desorption studies, it was found that acid sites of H-birnessite were predominantly Lewis acid in nature. Pyridine desorption studies showed that the Lewis band at 1601 cm^{-1} splits after heating at 200°C. Split bands were distinctly seen in H-birnessite samples at 1634 and 1613 cm^{-1}, indicating the presence of two types of Lewis acid sites having higher acid strength. During the decomposition reaction, formates with different adsorption structures and carbonates were formed as intermediates. During the heating process, the adsorbed formic acid species transformed into the formate species. The formate reacts with surface Lewis acid sites (Mn ions) or OH groups through the lone pair on the oxygen atom and releases a proton to form a carbonate that is finally transformed to CO. The enhancement of the carbonyl absorption (1740 cm^{-1}) at 300°C demonstrates that oxidation of surface formic acid occurs.

APPENDIX A: SUPPLEMENTARY DATA

The analyses of XRD. Supplementary data associated with this article can be found in the online version.

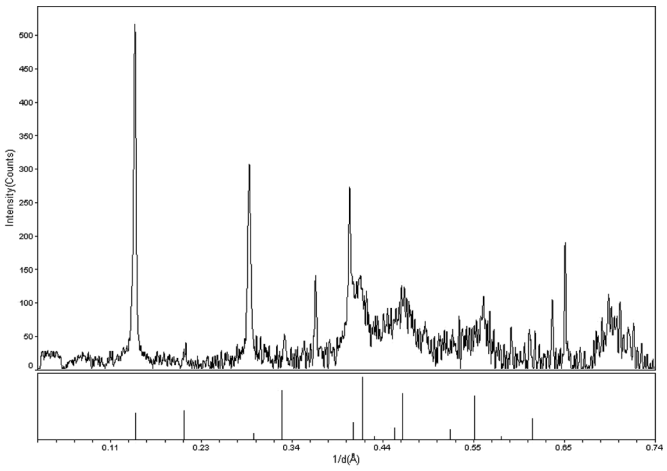

XRD pattern of K-birnessite

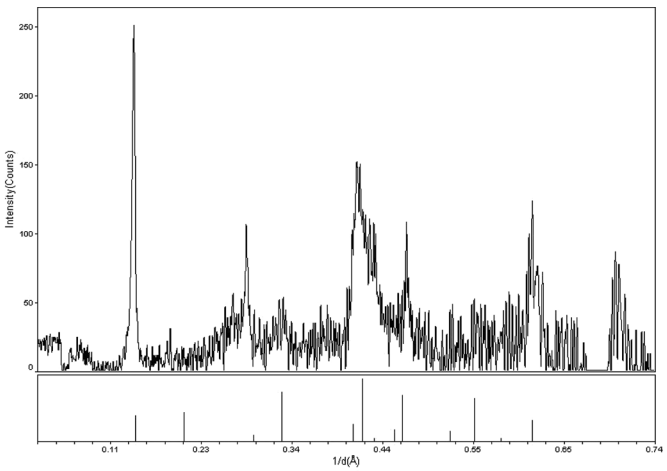

XRD pattern of H-birnessite

REFERENCES

1. Popova, G. Y.; Zakharov, I. I.; Andrushkevich, T. V. Mechanism of formic acid decomposition on P–Mo heteropolyacid. *React. Kinet. Catal. Lett.* **1999**, *66*, 251–256.
2. Lanson, B.; Drits, V. A.; Silvester, E.; Manceau, A. Structure of H-exchanged hexagonal birnessite and its mechanism of formation from Na-rich monoclinic buserite at low pH. *Am. Mineral.* **2000**, *85*, 826–838.
3. Gaillot, A.-C.; Lanson, B.; Drits, V. A. Structure of birnessite obtained from decomposition of permanganate under soft hydrothermal conditions. 1. Chemical and structural evolution as a function of temperature. *Chem. Mater.* **2005**, *17*, 2959–2975.
4. Gac, W. The influence of silver on the structural, redox and catalytic properties of the cryptomelane-type manganese oxides in the low-temperature CO oxidation reaction. *App. Catal. B Environ.* **2007**, *75*, 107–117.
5. El-Shobaky, G. A.; Fagal, G. A.; Ghozza, A. M.; Shouman, M. A. Surface and catalytic properties of manganese oxides supported on active alumina. *Mater. Lett.* **1994**, *19*, 225–231.
6. Kim, S. C.; Shim, W. G. Catalytic combustion of VOCs over a series of manganese oxide catalysts. *App. Catal. B Environ.* **2010**, *98*, 180–185.
7. Kang, M.; Park, E. D.; Kim, J. M.; Yie, J. E. Manganese oxide catalysts for NOx reduction with NH_3 at low temperatures. *Appl. Catal. A Gen.* **2007**, *327*, 261–269.
8. Li, B.; Xu, X.; Zhu, L.; Ding, W.; Mahmood, Q. Catalytic ozonation of industrial wastewater containing chloro and nitro aromatics using modified diatomaceous porous filling. *Desalination* **2010**, *254*, 90–98.
9. Aguero, F. N.; Scian, A.; Barbero, B. P.; Cadús, L. E. Combustion of volatile organic compounds over supported manganese oxide: influence of the support, the precursor and the manganese loading. *Catal. Today* **2008**, *133–135*, 493–501.
10. Ivanov, E. A.; Popova, G. Ya.; Chesalov, Yu. A.; Andrushkevich, T. V. In situ FTIR study of the kinetics of formic acid decomposition on V–Ti oxide catalyst under stationary and non-stationary conditions. Determination of kinetic constants. *J. Mol. Catal. A Chem.* **2009**, *312*, 92–96.
11. Jacobs, G.; Patterson, P. M.; Graham, U. M.; Crawford, A. C.; Davis, B. H. Low temperature water gas shift: the link between the catalysis of WGS and formic acid decomposition over Pt/ceria. *Int. J. Hydrogen Energ.* **2005**, *30*, 1265–1276.
12. Jacobs, G.; Patterson, P. M.; Graham, U. M.; Crawford, A. C.; Dozier, A.; Davis, B. H. Catalytic links among the water-gas shift, water-assisted formic acid decomposition, and methanol steam reforming reactions over Pt-promoted thoria. *J. Catal.* **2005**, *235*, 79–91.
13. Araña, J.; Garriga i Cabo, C.; Doña-Rodríguez, J. M.; González-DiôÇaz, O.; Herrera-Melián, J. A.; Pérez-Peña, J. FTIR study of formic acid interaction with TiO_2 and TiO_2 doped with Pd and Cu in photocatalytic processes. *Appl. Surf. Sci.* **2004**, *239*, 60–71.
14. Borowiak, M. A.; Jamróz, M. H.; Larsson, R. Catalytic decomposition of formic acid on oxide catalysts: III. IOM model approach to bimolecular mechanism. *J. Mol. Catal. A Chem.* **2000**, *152*, 121–132.
15. Zhao, G.; Joó, F. Free formic acid by hydrogenation of carbon dioxide in sodium formate solutions. *Catal. Commun.* **2011**, *14*, 74–76.
16. Millar, G. J.; Rochester, C. H.; Waugh, K. C. An FTIR study of the adsorption of formic acid and formaldehyde on potassium-promoted Cu/SiO_2 catalysts. *J. Catal.* **1995**, *155*, 52–58.
17. Li, X.; Pan, G.; Qin, Y.; Hu, T.; Wu, Z.; Xie, Y. EXAFS studies on adsorption–desorption reversibility at manganese oxide–water interfaces: II. Reversible adsorption of zinc on δ-MnO_2. *J. Colloid Interf. Sci.* **2004**, *271*, 35–40.
18. Parida, K. M.; Mallick, S.; Dash, S. S. Studies on manganese nodule leached residues: 2. Adsorption of aqueous phosphate on manganese nodule leached residues. *J. Colloid Interf. Sci.* **2005**, *290*, 22–27.
19. Julien, C. M. Local structure of lithiated manganese oxides. *Solid State Ionics* **2006**, *177*, 11–19.
20. Yang, R.; Wang, Z.; Dai, L.; Chen, L. Synthesis and characterization of single-crystalline nanorods of α-MnO_2 and γ-MnOOH. *Mater. Chem. Phys.* **2005**, *93*, 149–153.
21. Kang, L.; Zhang, M.; Liu, Z.-H.; Ooi, K. IR spectra of manganese oxides with either layered or tunnel structures. *Spectrochim. Acta A* **2007**, *67*, 864–869.
22. Yang, D. S.; Wang, M. K. Syntheses and characterization of birnessite by oxidizing pyrochroite in alkaline conditions. *Clays Clay Miner.* **2002**, *50*, 63–69.
23. Chakraborty, B.; Viswanathan, B. Surface acidity of MCM-41 by in situ IR studies of pyridine adsorption. *Catal. Today* **1999**, *49*, 253–260.
24. Jankovic, L.; Komadel, P. Metal cation-exchanged montmorillonite catalyzed protection of aromatic aldehydes with Ac_2O. *J. Catal.* **2003**, *218*, 227–233.
25. Shimizu, K.; Higuchi, T.; Takasugi, E.; Hatamachi, T.; Kodama, T.; Satsuma, A. Characterization of Lewis acidity of cation-exchanged montmorillonite K-10 clay as effective heterogeneous catalyst for acetylation of alcohol. *J. Mol. Catal. A Chem.* **2008**, *284*, 89–96.
26. Liu, L.; Feng, Q.; Yanagisawa, K.; Bignall, G.; Hashida, T. Lithiation reactions of Zn- and Li-birnessites in non-aqueous solutions and their stabilities. *J. Mater. Sci.* **2002**, *37*, 1315–1320.
27. Yang, L.-X.; Zhu, Y.-J.; Cheng, G.-F. Synthesis of well-crystallized birnessite using ethylene glycol as a reducing reagent. *Mater. Res. Bull.* **2007**, *42*, 159–164.
28. Kecskés, T.; Raskó, J.; Kiss, J. FTIR and mass spectrometric study of HCOOH interaction with $TiOi_2$ supported Rh and Au catalysts. *Appl. Catal. A Gen.* **2004**, *268*, 9–16 (referenced therein).
29. Flaherty, D. W.; Berglund, S. P.; Buddie Mullins, C. Selective decomposition of formic acid on molybdenum carbide: a new reaction pathway. *J. Catal.* **2010**, *269*, 33–43.
30. Miller, K. L.; Lee, C. W.; Falconer, J. L.; Medlin, J. W. Effect of water on formic acid photocatalytic decomposition on TiO_2 and Pt/TiO_2. *J. Catal.* **2010**, *275*, 294–299.
31. Glisenti, A. Interaction of formic acid with Fe_2O_3 powders under different atmospheres: an XPS and FTIR study. *J. Chem. Soc. Faraday Trans.* **1998**, *94*, 3671–3676.
32. Huang, J. Y.; Huang, H. G.; Lin, K. Y.; Liu, Q. P.; Sun, Y. M.; Xu, G. Q. The structures of physisorbed and chemisorbed formic acid on Si(1 1 1)-7 $\times$ 7. *Surf. Sci.* **2004**, *549*, 255–264.
33. Chen, T.; Wu, G.; Feng, Z.; Hu, G.; Su, W.; Ying, P.; Li, C. In situ FT-IR study of photocatalytic decomposition of formic acid to hydrogen on Pt/TiO_2 catalyst. *Chinese J. Catal.* **2008**, *29*, 105–107.
34. Farias, A. M. D.; Barandas, A. P. M. G.; Perez, R. F.; Fraga, M. A. Water-gas shift reaction over magnesia-modified Pt/CeO_2 catalysts. *J. Power Sources* **2007**, *165*, 854–860.
35. Brownson, J. R. S.; Tejedor, M. I.; Anderson, M. A. Photoreactive anatase consolidation characterized by FTIR spectroscopy. *Chem. Mater.* **2005**, *17*, 6304–6310.
36. Rotzinger, F. P.; Truttmann, J. M. K.; Hug, S. J.; Shklover, V.; Gratzel, M. Structure and vibrational spectrum of formate and acetate adsorbed from aqueous, solution onto the TiO_2 rutile (110) surface. *J. Phys. Chem. B* **2004**, *108*, 5004–5017.
37. Dolamic, I.; Burgi, T. Photoassisted decomposition of malonic acid on TiO_2 studied by in situ attenuated total reflection infrared spectroscopy. *J. Phys. Chem. B* **2006**, *110*, 14898–14904.
38. Brownson, J. R. S.; Tejedor, M. I.; Anderson, M. A. FTIR spectroscopy of alcohol and formate interactions with mesoporous TiO_2 surfaces. *J. Phys. Chem. B* **2006**, *110*, 12494–12499.